Int. J. Therm. Sci. (2001) 40, 595–602

S1290-0729(01)01250-9/FLA

Subcritical oscillatory instability in porous beds

Mustapha Mbaye [a], Earl Bilgen [b]

[a] *Shaped Castings Platform, Alcoa Technical Center 100 Technical Drive, Alcoa Center, PA 15069-0001, USA*

[b] *Mechanical Engineering Department, Ecole Polytechnique, C.P. 6079, Centre Ville, Montreal, Pc H3C 3A7, Canada*

(Received 19 May 2000, accepted 14 September 2000)

Abstract — This paper presents a study of the stability of gas flow subject to an adverse temperature and concentration gradient. The onset and the development of convection were studied using a numerical technique and the analytical linear and nonlinear stability theories. The range covered, for a unity aspect ratio and $\Omega = \varepsilon/\sigma$, was $R_C Le = 20$ and 40 with $Le = 0.5 - 10$. The thermal Rayleigh number was chosen as the bifurcation parameter and the range covered was from 0 to 150. Numerical solutions of the set of governing equations show a symmetrical steady and oscillating mode in subcritical flows. A bifurcation phenomenon was found, which showed the existence of two symmetrical branches. Steady state convection can be developed below the critical value R_T^c predicted by the linear theory. This study has demonstrated that the presence of two diffusing components (heat and mass) with different diffusivities can lead to the development of subcritical oscillating instabilities in the range $4\pi + \xi \leq R_T \leq R_T^c - \xi'$. © 2001 Éditions scientifiques et médicales Elsevier SAS

thermosolutal convection / double diffusion / instability / porous media

Nomenclature

A	aspect ratio $= H/L$	
C	dimensionless concentration $= (C_0' - C')/\Delta C'$	
C'	concentration	$\mathrm{mol\cdot m^{-3}}$
c	heat capacity	$\mathrm{J\cdot kg^{-1}\cdot K^{-1}}$
D	mass diffusivity	$\mathrm{m^2\cdot s^{-1}}$
g	gravitational acceleration	$\mathrm{m\cdot s^{-2}}$
H	height of the cavity	m
h	convective heat transfer coefficient	$\mathrm{W\cdot m^{-2}\cdot K^{-1}}$
K	permeability	$\mathrm{m^2}$
k	thermal conductivity of the fluid filled medium	$\mathrm{W\cdot m^{-1}\cdot K^{-1}}$
L	width of the cavity	m
Le	Lewis number $= \alpha_T/D$	
Nu	Nusselt number $= \frac{\overline{h}L}{k}$	
p'	pressure	Pa
R_C	concentration Rayleigh number $= g\beta_C \Delta C' K L/(\nu D)$	
R_T	thermal Rayleigh number $= g\beta_T \Delta T' K L/(\nu \alpha_T)$	
T'	temperature	K
S	surface element	
t'	time	s
x', y'	Cartesian coordinates	m
x, y	dimensionless coordinates in x, y direction, x'/L, y'/L	
$\mathcal{V}$	volume element	

Greek symbols

α_T	thermal diffusivity $= k/(\rho c_p)$	$\mathrm{m^2\cdot s^{-1}}$
β_C	concentration expansion coefficient	$\mathrm{K^{-1}}$
β_T	thermal expansion coefficient	$\mathrm{K^{-1}}$
$\Delta T'$	temperature difference $= T_2' - T_1'$	K
$\Delta C'$	concentration difference $= C_2' - C_1'$	$\mathrm{mol\cdot m^{-3}}$
ε	normalized porosity	
σ	fluid heat capacity ratio	
Ω	porosity-heat capacity ratio	
θ	dimensionless temperature $= (T' - T_o')/\Delta T'$	
μ	dynamic viscosity	$\mathrm{kg\cdot m^{-1}\cdot s^{-1}}$
ν	kinematic viscosity	$\mathrm{m^2\cdot s^{-1}}$
ρ	fluid density	$\mathrm{kg\cdot m^{-3}}$
ψ'	stream function	$\mathrm{m^2\cdot s^{-1}}$
ψ	dimensionless stream function $= \psi'/\alpha$	

Subscript

eff	effective

E-mail address: bilgen@meca.polymtl.ca (E. Bilgen).

ext extremum
f fluid medium
i initial condition
max maximum
min minimum
o reference

Superscript

′ dimensional variables
c critical

1. INTRODUCTION

Thermosolutal convection is present in many industrial processes [1], especially those involving phase change phenomena such as melting-solidification, solid-gas reactions [2, 3]. For example, hydrogen diffuses in solidifying liquid metals and creates porosity defects that substantially reduces the metal's ductility and leads to premature fractures. The alloying elements can also diffuse and macrosegration can occur in solidifying alloys due to the double diffusion of heat and mass. The bibliography reveals a great number of studies on this subject, due to the industrial and technological importance of applications such as industrials processing, oceanography, solid-gas thermochemical systems, adsorption systems, building insulation, underground disposal of contaminants and fog formation [1]. These systems involve double diffusive flows with or without reactions. For example, the main problem of chemical reactors is to maintain the nonconvectivity of the reactive zone and its stability to guaranty good performance. This shows the great importance of the thermosolutal convection in porous beds [2]. Since the diffusivities of these two components are quite different, instabilities of the double diffusive type may occur and lead to multiple steady convective solutions. Many studies have been done with the vertical porous enclosure [4] and the existence of multiple steady states for opposing flows has been already demonstrated [5].

The thermosolutal convection in enclosures may be classified according to the order of magnitude of the Lewis number [6]. The range of large value Lewis number (order of magnitude 10^2) refers to thermosolutal convection in liquids and small numbers to double diffusion in binary gases. The latter is encountered in various applications, such as, in contaminant transport in groundwater, solar ponds and solid-gas chemical reactors. The literature review shows that this case has not been addressed. Its special feature is to understand the dynamic behaviour of the solid-gas fixed bed reactor whom the performance limitations are due to heat and mass transfer [3]. The first aim is to determine the critical conditions of the onset of convection which is not desirable in such chemically reacting systems. It is important to know the presence of instabilities as well as oscillating instabilities.

The present study is concerned with problems where the Lewis number is in the range of $1 \leq Le \leq 10$. The thermosolutal natural convection due to vertical temperature and concentration gradients in horizontal layers without reaction will be investigated and the critical conditions for the onset of convection will be determined.

2. PROBLEM AND MATHEMATICAL FORMULATION

The considered system to be analyzed is presented in *figure 1*. We consider a saturated porous layer with a void fraction ε, bounded by two dimensional planar channel of height H and width L. The lower plane of the system is maintained at higher constant temperature T_1' and higher concentration C_1', the upper plane at lower constant temperature T_2' and lower concentration C_2'. The lateral walls are impermeable and perfectly insulated, so that the system can be considered adiabatic. The solute will enter the system by diffusion through the lower plane while it will leave the system through the upper plane. It should be noted that the basic problem concerns two diffusing components, heat and mass (solute, gas or liquid).

The fluid is considered Newtonian and incompressible, and all thermophysical properties are constant except for the density variations in the buoyancy term as modeled by the Boussinesq approximation. Assuming the Dufour and Soret effects negligible and the validity of two-dimensional Darcy's laminar flow in an homogeneous and isotropic medium, the governing equations become:

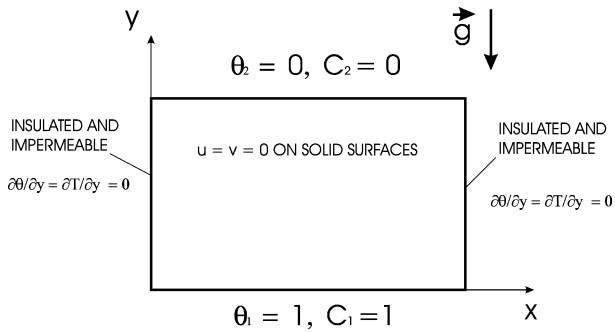

Figure 1. Schematic of the problem with boundary conditions.

State equation:

$$\rho = \rho_0\left[1 - \beta_T\left(T' - T_0'\right) - \beta_C\left(C_0' - C'\right)\right] \qquad (1)$$

where $\beta_T > 0$ and $\beta_C > 0$ are the thermal and concentration expansion coefficients as defined in [7]. The reference temperature and concentration are respectively: $T_0' = T_1'$ and $C_0' = C_1'$.

Mass balance:

$$\Omega\frac{\partial C}{\partial t} + J[C,\psi] = \frac{1}{Le}\nabla\cdot\nabla C \qquad (2)$$

Energy balance:

$$\frac{\partial T}{\partial t} + J[T,\psi] = \nabla^2 T \qquad (3)$$

Momentum balance:

$$\nabla^2\psi = -R_T\frac{\partial T}{\partial}x - R_C\frac{\partial C}{\partial x} \qquad (4)$$

where $\vec{V}$ is the dimensionless filtration velocity with components $u = \frac{\partial\psi}{\partial x}$, $v = -\frac{\partial\psi}{\partial y}$, and J is the Jacobian defined by

$$J[f,g] = \frac{\partial f}{\partial x}\frac{\partial g}{\partial y} - \frac{\partial f}{\partial y}\frac{\partial g}{\partial x} \qquad (5)$$

The boundary conditions are shown in *figure 1* and the initial conditions are $(T, C, \psi) = (T_i, C_i, \psi_i)$ at $t = 0$. The initial conditions were chosen depending of the simulations performed. The following scaling parameters are used to obtain the above dimensionless equations:

$$t = t'\frac{\alpha_{\text{eff}}}{L^2\sigma}, \qquad (x,y) = \frac{(x,'y')}{L},$$
$$p = p'\frac{K}{\mu_f\alpha_{\text{eff}}}, \qquad A = \frac{H}{L},$$
$$\vec{V} = \vec{V}'\frac{L}{\alpha_{\text{eff}}}, \qquad C = \frac{C_0' - C'}{\Delta C'},$$
$$\theta = \frac{T' - T_0'}{\Delta T'}, \qquad \sigma = \frac{(\rho c)_{\text{eff}}}{(\rho c_p)_f},$$
$$\Omega = \frac{\varepsilon}{\sigma}, \qquad R_T = \frac{g\beta_T L K\Delta T'}{\nu\alpha_T},$$
$$R_C = \frac{g\beta_C L K\Delta C'}{\nu D}, \qquad Le = \frac{\alpha_T}{D}$$

From equations (1)–(4), it appears that the problem is governed by the following parameters: the Rayleigh numbers R_T and R_C, the Lewis number Le, the aspect ratio A and the initial conditions (T_i, C_i, ψ_i). The parameters $\Omega = 1$ and $A = 1$ are kept constant in all simulations.

The average Nusselt and Sherwood numbers are calculated at the cold and heated sides. The heat and mass fluxes were calculated by a Taylor expansion with four points. The integration was evaluated by a combination of Simpson's 1/3 and 3/8 rules for an odd number of intervals. For an even number, only the 1/3 rule is used, which normally gives a better accuracy.

3. NUMERICAL SOLUTION

The conservation equations (2)–(4) describing the concentration, temperature and flow field in this problem were solved numerically using a finite-difference discretization procedure. Central-difference formulae were used for all spatial derivative terms. A modified alternate direction implicit procedure was used to solve the energy equation. The finite-difference forms of energy equation is written in conservative form for the convective terms to preserve the conservative form property [8]. The stream function equation is solved by a successive over-relaxation method. The velocity field is obtained by integration of the stream function.

The boundary conditions for the energy equation in differential form may be written in finite difference form employing one-sided differences or a fictitious grid point outside the region. However, greater accuracy and often more flexibility is obtained by considering the grid control volume which ensures, for a surface grid point, the energy and mass conservation. The energy equation (3) is integrated in the first control volume of the boundary. After applying the divergence theorem the final equation is:

$$\Omega\frac{\partial}{\partial t}\int_{\mathcal{V}} T\ \mathrm{d}\mathcal{V} + \int_S \vec{V}T\ \vec{\mathrm{d}}S = \frac{1}{Le}\int_S \nabla T\ \vec{\mathrm{d}}S \qquad (6)$$

where $\mathcal{V}$ and S are respectively the volume and the surface of element.

The iterative convergence of the stream function, temperature and concentration is checked by comparing two successive iterations n and $n+1$ at any node. The convergence criterion was chosen such that $\max|(f^{n+1} - f^n)/f^n| < 10^{-5}$ where f represents T, C or Ψ. The steady state was reached when the maximum of the fractional changes in the stream function's extremum values ψ_{ext}, ($\psi_{\max}$ or $\psi_{\min}$), the Nusselt and

Sherwood numbers between a time step k and $k-10$ is less than 10^{-10}. To achieve the desired accuracy and the numerical stability, a small time step ($\Delta t = 10^{-3}$–10^{-4}) was used. The discretization scheme of the governing equations is second-order accurate. The uniform mesh sizes were used for both x and y directions and were varied from 41×41 to 81×81 depending on the strength of convection. The results found in [4, 5] are reproduced successfully.

4. ANALYTICAL SOLUTIONS

From the governing equations (1)–(4), the dimensionless parameters that characterize the physics, are identified: A, Ω, Le, R_T and R_C. To validate the numerical study, the analytical solution using linear and nonlinear stability theories was carried out. As in the case of the numerical study, the parameters A and Ω were kept constant and equal to one, while the other three, Le, R_T and R_C were taken as variable parameters.

4.1. Linear stability theory

From the static state (no motion, $\psi = 0$; pure heat and mass conduction), infinitesimal perturbations may either grow or be dampened depending of the value of the governing parameters (Le, R_T, R_C). Assuming the solution for the state of rest (ψ_0, T_0, C_0), an infinitesimal perturbation (ψ_1, T_1, C_1) applied to the basic state gives

$$\begin{cases} \psi = \psi_0 + \psi_1, \\ T = T_0 + T_1, \\ C = C_0 + C_1 \end{cases} \tag{7}$$

By introducing this solution into the governing equations, one obtains

$$\begin{cases} \Delta\psi_1 = -R_T \dfrac{\partial T_1}{\partial x} - R_C \dfrac{\partial S_1}{\partial x}, \\ \dfrac{\partial T_1}{\partial t} + J[T_1, \psi_1] = \nabla^2 T_1, \\ \Omega \dfrac{\partial C_1}{\partial t} + J[C_1, \psi_1] = \dfrac{1}{Le}\nabla^2 C_1 \end{cases} \tag{8}$$

where $\Omega = 1$ and it may be shown as variable in the equations.

The solution to the perturbation equations (8) are sought as expansion of the following trial functions

$$\begin{cases} \Psi_1 = \exp(\lambda t) \sin \dfrac{\pi x}{A} \sin \pi y, \\ T_1 \sim \exp(\lambda t) \cos \dfrac{\pi x}{A} \sin \pi y, \\ C_1 \sim \exp(\lambda t) \cos \dfrac{\pi x}{A} \sin \pi y \end{cases} \tag{9}$$

The substitution of these functions into equations (8) results in a solution of the equation of the form

$$\lambda^2 + b\lambda + c = 0 \tag{10}$$

Depending on the value of (b, c), equation (10) may have either complex or real roots, and the complex roots may have negative or positive real parts.

(1) Single positive real root, if

$$R_T > R_1 = 4\pi^2 + LeR_C \tag{11}$$

This represents the smallest thermal Rayleigh number, R_T, under which the stability is guaranteed for $Le = 1$.

(2) If $R_C > R_C^0 = \frac{4\pi^2}{Le(\Omega Le - 1)}$ there will be two possibilities

(a) There will be two positive real roots, if

$$\begin{cases} R_1 \geq R_T \geq R_2, \\ R_2 = \big(4\pi^2(\Omega Le - 1) + LeR_C \\ \qquad + 4\pi[LeR_C(\Omega Le - 1)]^{1/2}\big)/(\Omega Le) \end{cases} \tag{12}$$

(b) there will be two conjugate complex roots with a positive real part, if

$$\begin{cases} R_2 > R_T \geq R_3, \\ R_3 = 4\pi^2\left(1 + \dfrac{1}{\Omega Le}\right) + \dfrac{R_C}{\Omega} \end{cases} \tag{13}$$

These results show that the system will be stable only if $R_T \leq \min(R_1, R_3)$. In this case, a small perturbation will be annealed. If $R_T > \min(R_1, R_3)$, it will be unstable. It is noted however that the linear stability analysis does not show the subcritical instabilities. Using a nonlinear analysis, it will be shown that it may be unstable under the linear stability limit, as it was found in the numerical solutions.

4.2. Nonlinear stability theory

Using the Lorentz model, we can solve the governing equations (8) of the perturbed state (ψ_1, T_1, C_1). The

perturbed variables can be approximated by a minimal Fourier representation as,

$$\begin{cases} \Psi_1 \sim \phi(t)\sin\pi x \sin\pi y, \\ T_1 \sim F_1(t)\cos\pi x \sin\pi y + F_2(t)\sin\pi y, \\ C_1 \sim G_1(t)\cos\pi x \sin\pi y + G_2(t)\sin\pi y \end{cases} \tag{14}$$

These trial functions reduce the perturbed equations to five transient ordinary differential equations with five unknown variables (ϕ, F_i, G_i, $i = 1, 2$). Then the steady solution can be obtained for ϕ, F_i and G_i as

$$\begin{cases} \phi = \pm\dfrac{1}{4}\left[\dfrac{-b \pm \sqrt{b^2 - 4c}}{2}\right]^{1/2}, \\ F_1 = -\dfrac{1}{2\pi}\phi\left[1 + \dfrac{\phi^2}{16}\right]^{-1}, \\ F_2 = \dfrac{1}{8}\phi F_1, \\ G_1 = -\dfrac{Le}{2\pi}\phi\left[1 + \dfrac{Le^2\phi^2}{16}\right]^{-1}, \\ G_2 = \dfrac{1}{8}\phi G_1 \end{cases} \tag{15}$$

The values of (b, c) are given by

$$b = \frac{1}{4\pi^2}\left[4\pi^2\left(1 + Le^{-2}\right) + \frac{R_C}{Le} - R_T\right],$$
$$c = \frac{1}{4\pi^2 Le}\left(4\pi^2 + R_C Le - R_T\right)$$

The above solution shows the possibility of subcritical instabilities, which means that convection may arise at $R_T < R_1$ if

$$\begin{cases} R_C > R_C^{0,\text{nonlinear}} = \dfrac{4\pi^2}{Le(Le^2 - 1)} \\ R_T > R_2^{\text{nonlinear}}, \\ \quad = \dfrac{4\pi(Le - 1) + LeR_C + 4\pi\sqrt{LeR_C(Le^2 - 1)}}{Le^2} \end{cases} \tag{16}$$

By comparing both theories, it is clear that the domain of nonlinear stability is smaller than the one predicted by the linear stability theory. The above solutions are used to understand the instabilities found with the numerical analysis.

5. RESULTS AND DISCUSSION

Typical numerical experiments were carried out covering the range $0 \le R_T \le 150$ for a unity aspect ratio and $\Omega = \varepsilon/\sigma$, and $R_C Le = 20$ and 40 corresponding to $Le = 0.5$, 1, 2, 5 and 10. Thus the space (R_C, Le, R_T) was studied and the thermal Rayleigh number, R_T, was chosen as the bifurcation parameter. For all experiments, the curves were obtained by increasing or decreasing respectively the thermal Rayleigh number, R_T value from 0 to 150 or from 150 to 0. The initial conditions for the first run were the rest state and those of the decreasing branch were initiated from steady clockwise (or counterclockwise) solutions of higher ($R_T = 250$) values. All subsequent runs were performed with initial conditions being at the previous state.

The branch of steady solutions

The solutions were obtained by increasing (left arrow in *figures 2* and *3*) or decreasing (right arrow in *figures 2* and *3*) the value of R_T by a variable step size ($\Delta R_T = 0.01$–2) depending on the difficulties in obtaining a steady state. The number of circles indicates the number of cells obtained. The steady solutions are symmetrical: the above and below branches correspond respectively to the counterclockwise (positive) and clockwise (negative) motions. *Figures 2* and *3* show the extremum stream function values as a function of the thermal Rayleigh number, R_T for different values of the Lewis number, Le. From rest states, one cell was obtained

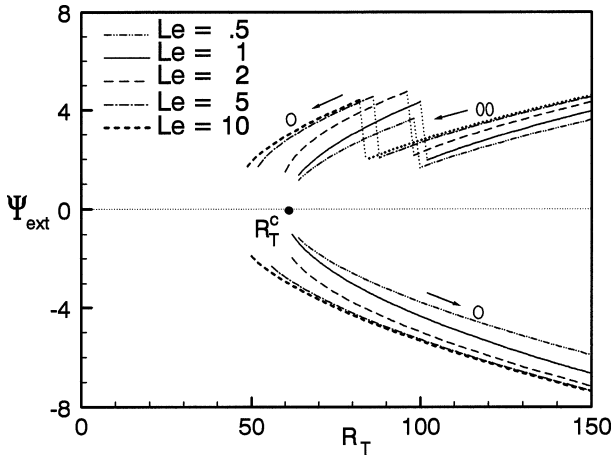

Figure 2. Extremum stream function as a function of the thermal Rayleigh number for $R_C Le = 20$ and various Le. o and oo show the number of cells.

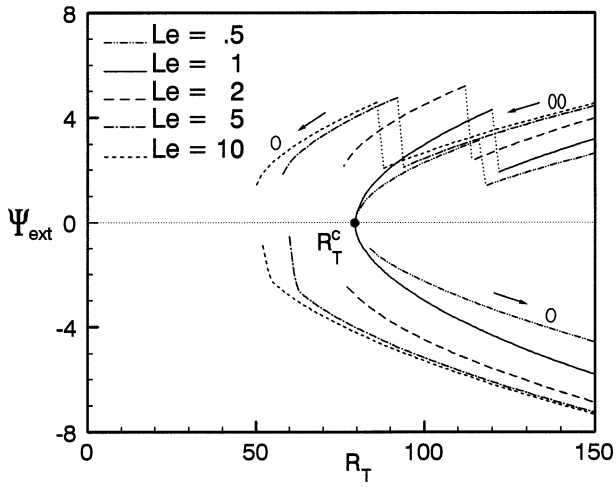

Figure 3. Extremum stream function a function of the thermal Rayleigh number for $R_C Le = 40$ and various Le. o and oo show the number of cells.

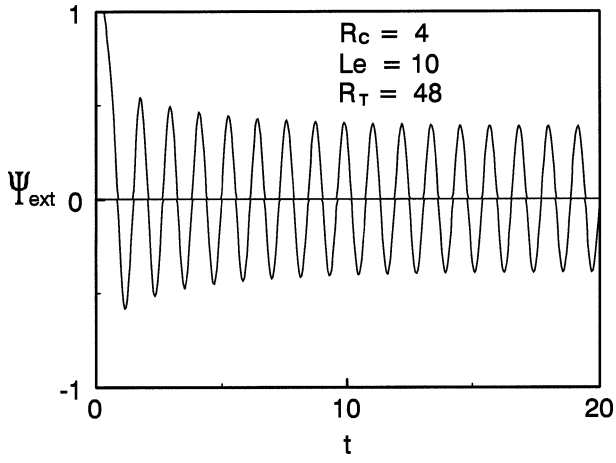

Figure 4. Amortized oscillation flow for $R_C = 4$, $Le = 10$, $R_T = 48$ presented in the plane of the extremum stream function and time.

above the critical value $R_T^c = 4\pi + R_C Le$ and steady state solution was obtained until the final value of R_T. When decreasing R_T from two symmetrical (positive and negative) steady solutions, a branch of two cells which rotate in the opposite direction was obtained. For the case of $Le = 10$ in *figure 2*, as expected, the branch coming down from $R_T = 150$ remains stable until $R_T = 80$. Below this value, a steady unicellular positive flow was obtained until $R_T \simeq 50$ but below the critical Rayleigh number, R_T^c, an oscillating flow was found at $R_T = 46$. In *figure 3*, for $Le = 10$ and $R_T = 48$ ($< R_T^c$), an oscillating flow occured. The solutions found became steady or sustained oscillating state. *Figure 4* shows that the amplitude and

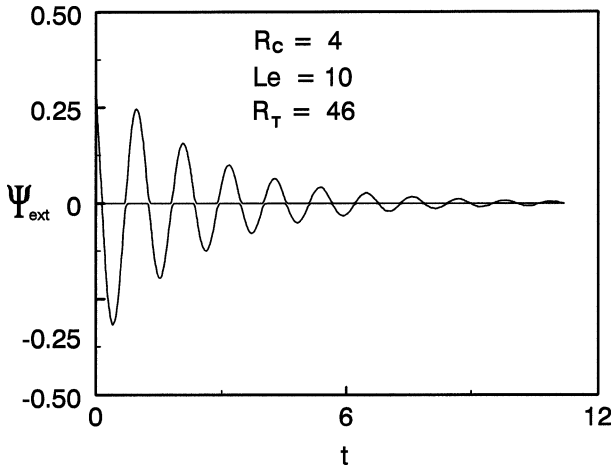

Figure 5. Amortized oscillation flow for $R_C = 4$, $Le = 10$, $R_T = 46$ presented in the plane of the extremum stream function and time.

the frequency of oscillations are constant after a dimensionless time less than 8. For a smaller $R_T = 46$ the oscillation was amortized after $t < 12$ as shown in *figure 5*. The same study was carried out with $R_C Le = 20$ (presented in *figure 2*) and 40 (presented in *figure 3*). The general conclusion is that the oscillation mode in a subcritical state was arrived only for $Le = 2$, 5 and 10 and below their respective critical values, R_T^c, predicted by the linear theory. In the range $46 \leq R_T \leq 80$, both oscillating and steady convective states are present and occur in the decreasing branch. In general, instabilities occur around the values less than the critical value, $R_T < R_T^c$, but also at greater than the critical values, $R_T > 4\pi^2$, for the onset of Bénard convection in a system with only thermal effect. At small R_T values, there are multiple stable or unstable steady solutions. The simulations performed show that unstable solutions occur in the range $4\pi + \xi \leq R_T \leq R_T^c - \xi'$, where ξ and ξ' are values which can be determined more precisely by an analytical method.

Flow, heat and mass structures

A bifurcation phenomenon is found in the double diffusive flows within the enclosure with both temperature and concentration gradients. A steady state convection can be developed below the critical value R_T^c. This fact shows the possibility of development of subcritical steady flows. *Figure 6* shows the streamlines, isotherms and isoconcentrations of the steady state for $R_C Le = 20$, $R_T = 140$ for different values $Le = 0.5$, 1, and 10. Due to high Le, the solute boundary layer is much thinner than the thermal boundary layer. It is also developed at much

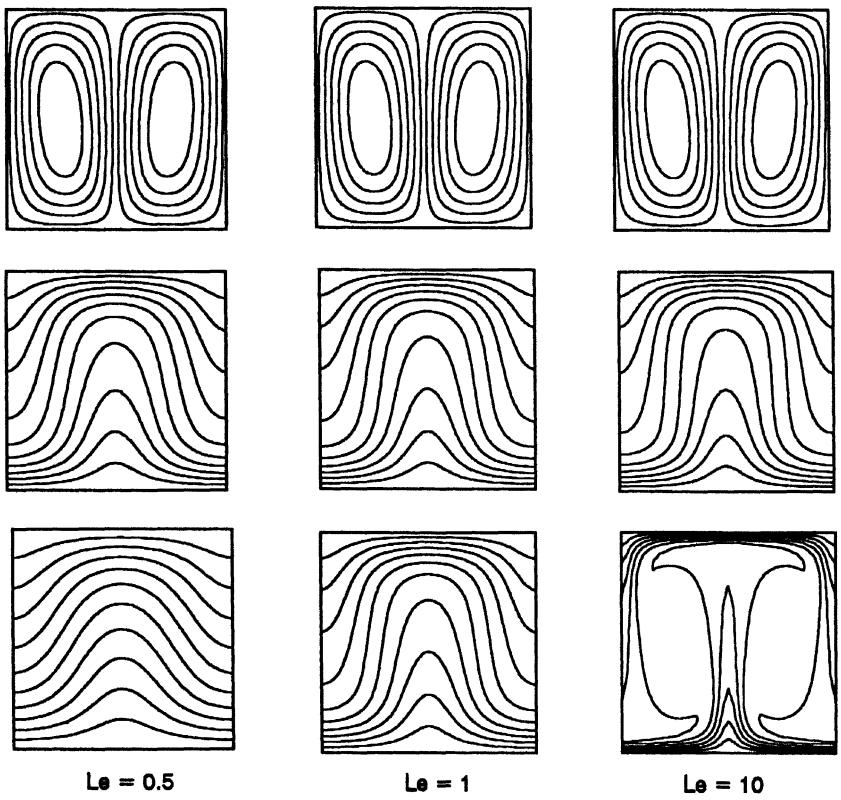

Figure 6. Streamlines (top), isotherms (middle) and isoconcentration (bottom) for $R_C Le = 20$ and $R_T = 140$, and for various Le. Isotherms are $\theta = 1$ at the lower plane and 0 at the upper, with 0.1 increment. Isoconcentrations, C are similarly, from 1 at the lower plane to 0 at the upper with 0.1 increment.

lower Rayleigh numbers. As expected, for $Le \to \infty$, the thickness of solute boundary becomes smaller and the concentration is well stratified in the core region. On the other hand, the temperature field shows that it is almost a conductive mode. The main point of this study is that, when $Le \to \infty$, convection can arise for $R_T > 4\pi^2$, which is the critical value for the onset of Bénard convection in purely thermal systems.

6. CONCLUSION

A study of the stability of gas flow subject to an adverse temperature and concentration gradient has been carried out. The onset and the development of convection were studied by numerical solutions of the set of complete governing equations as well as using the linear and nonlinear stability theories. It is shown that a steady and oscillating mode can also arise in subcritical flows. A bifurcation phenomena was found which shows the existence of two symmetrical branches. Steady state convection can be developed below the critical value R_T^c predicted by the linear theory. This study has demonstrated that the presence of two diffusing components of heat and mass with different diffusivities can lead to the development of subcritical oscillating instabilities in the range $4\pi + \xi \leq R_T \leq R_T^c - \xi'$. Numerical simulations as well as analytical solutions confirm the existence of subcritical regions in the vicinity of the critical Rayleigh number, R_T^c. These findings show that in some industrial processes undesired convection may appear, which may be detrimental to process efficiency and performance.

REFERENCES

[1] Cussler E.L., Diffusion Mass Transfer in Fluid Systems, 2nd edn., Cambridge Univ. Press, Cambridge, 1997.

[2] Gatica J.E., Viljoun H.J., Hlavacek V., Interaction between chemical reaction and natural convection in porous media, Chemical Engrg. Sci. 44 (9) (1989) 1853–1870.

[3] Mbaye M., Aidoun Z., Valkov V., Legault A., Analysis of chemical heat pumps (CHPS): basic concepts and numerical model description, Appl. Thermal Engrg. 18 (3–4) (1998) 131–146.

[4] Trevisan O.V., Bejan A., Mass and heat transfer by natural convection in a vertical slot filled with porous medium, Internat. J. Heat Mass Transfer 29 (3) (1986) 403–415.

[5] Mamou M., Vasseur P., Bilgen E., Multiple solutions for double-diffusive convection in a vertical porous enclosure, Internat. J. Heat Mass Transfer 38 (10) (1995) 1787–1798.

[6] Bennacer R., Godin D., Cooperating thermosolutal convection in enclosures-1. Scale analysis and mass transfer, Internat. J. Heat Mass Transfer 39 (13) (1996) 2671–2681.

[7] Giestas M., Pina H., Joyce A., The influence of radiation absorption on solar pond stability, Internat. J. Heat Mass Transfer 39 (18) (1996) 3873.

[8] Roache P.J., Computational Fluid Dynamics, Hermosa Publishers, Albuquerque, NM, 1982.